Supporting Information

Biagini et al. 10.1073/pnas.1205651109

SI Materials and Methods

Generation of CK-2–68–Resistant *Plasmodium falciparum* and Sequencing of the *Plasmodium falciparum* NDH2 Gene. *Plasmodium falciparum* K1 strain was incubated for 2 d with an IC_{90} concentration of CK-2–68 followed by withdrawal of the drug for 5 d. The procedure was repeated for several cycles until parasites became threefold resistant compared with wild type. The *Plasmodium falciparum* NDH2 (PfNDH2) gene of the CK-2–68–resistant strain was amplified from genomic DNA using the following primers: forward 5′-CCGCATGCCTATAATGTAGCAAAAAAATAATTT-3′ (SphI, underlined), reverse 5′-TTGAATTCTCATTTGATGAAAGGACGCCCATACCATTT-3′ (EcoRI, underlined). The forward primer generates a mature sequence starting at Tyr24 that excludes the mitochondrial leader sequence. The PCR was performed in a 50-µL volume containing ∼100 ng genomic DNA, 0.6 µM of each primer, 1 mM magnesium sulfate (Sigma), 0.3 mM deoxynucleotide triphosphate (Invitrogen), 10 µL Pfx amplification buffer (Invitrogen), and 1 unit Platinum Pfx DNA polymerase (Invitrogen). The reaction was performed using a Bio-Rad iCycler using the following parameters: a denaturation cycle of 94 °C for 3 min followed by 30 cycles of 94 °C for 15 s, 55 °C for 30 s, and 68 °C for 3 min, and a final cycle of 68 °C for 10 min.

The resultant ∼1.6-kb PCR product was agarose gel purified before insertion into pCR-Blunt vector (Invitrogen) and transformation into the TOP10 *Escherichia coli* cell strain. Plasmid DNA was extracted from successful transformants, and the incorporated PfNDH2 gene was fully sequenced at Cogenics using in-house M13 forward and reverse primers.

Metabolite Analysis in Drug-Treated Parasites. A Luna aminopropyl column (250 × 2 mm with a 5-µm particle size; Phenomenex) was used for the metabolites separation using an Accela Autosampler HPLC system (Thermo Fisher Scientific). The mobile phase consisted of solvent A [20 mM ammonium acetate + 20 mM ammonium hydroxide in 95:5 water:acetonitrile (pH 9.45)] and solvent B (acetonitrile). The gradients were as follows: $t = 0$, 15% A; $t = 7$ min, 100% A; $t = 14$ min, 100% A; $t = 16$ min, 15% A; $t = 35$ min, 15% A. Injection volume, flow rate, column temperature, and autosampler temperature were set at 20 µL, 150 µL/min, 15 °C, and 15 °C, respectively.

A TSQ Quantum Access Triple-Stage Quadrupole mass spectrometer (Thermo Electron Corporation) was used for the metabolite detection. Electrospray ionization spray voltage was 3,200 V. N_2 was used as sheath gas at 50 psi and as the auxiliary gas at 10 psi, and Ar was used as the collision gas (1.5 mTorr, 320 °C capillary temperature). Scan time for each single-reaction monitoring (SRM) event transition was 0.1 s with a scan width of 1 *m/z*. The instrument control, data acquisition, and data analysis were achieved applying Xcalibar (Thermoscientific) software. Metabolite concentration levels were quantified by applying a standard curve using a known concentration of standards for each of the 35 SRMs. The signal for each metabolite was defined as the area under the curve of the integrated peak. Each metabolite signal was normalized to the signal of the internal standard DL-arabinose (negative mode) or β-alanine (positive mode) in the same sample. All data were expressed as the normalized levels of a metabolite in the sample at time point to the number of trophozoite-stage parasites in untreated and drug-treated experiments. The ratio of drug-treated/untreated was log2-transformed and was visualized by making heat maps using MetaboAnalyst web server (1).

1. Xia J, Psychogios N, Young N, Wishart DS (2009) MetaboAnalyst: A web server for metabolomic data analysis and interpretation. *Nucleic Acids* Res 37(Web Server issue): W652–660.

Fig. S1. General synthesis of 3-methyl quinolones.

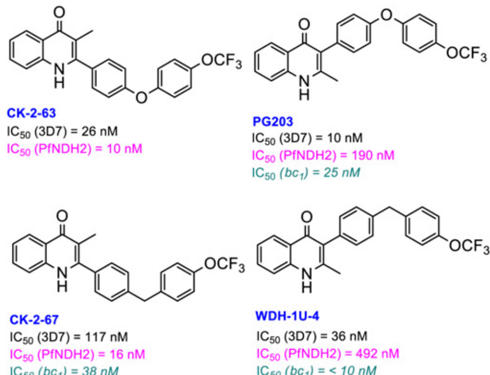

Fig. S2. The 2-aryl quinolones provide greater levels of PfNDH2 inhibition, whereas 3-aryl quinolones have high levels of bc_1 inhibition.

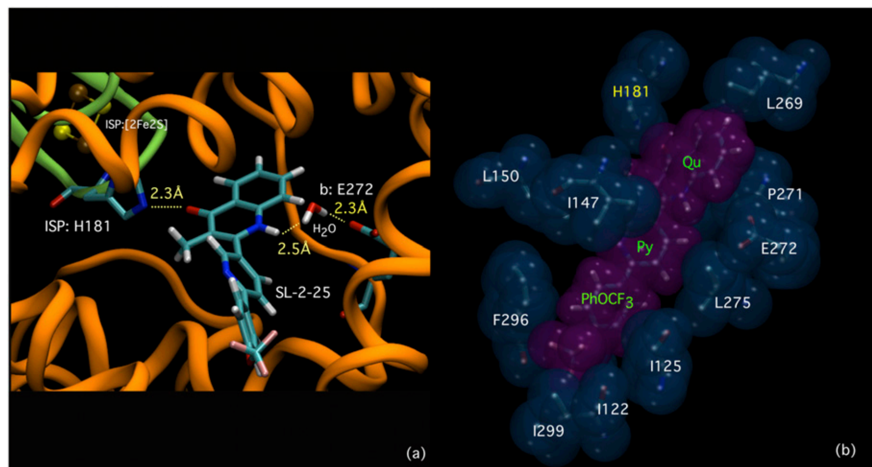

Fig. S3. (*A*) SL-2–25 docked within the Q_o site of yeast cytochrome bc_1 (Protein Data Bank code 3CX5). The a-carbon backbones of cytochrome *b* and the Rieske protein are represented in cartoon form in orange and green, respectively. Hydrogen bonds between SL-2–25 and the side chains of Glu272 (cytochrome *b*) and His181 (Rieske) are indicated by yellow dotted lines. (*B*) Predicted binding interactions between SL-2–25 and the Q_o site of the yeast bc_1 complex. Cytochrome *b* residues are labeled in white, and Rieske protein residues are labeled in yellow. The quinolone, pyridinyl, and trifluoromethoxyphenyl moieties of SL-2–2-5 are labeled “Qu,” “Py,” and “PhOCF3,” respectively.

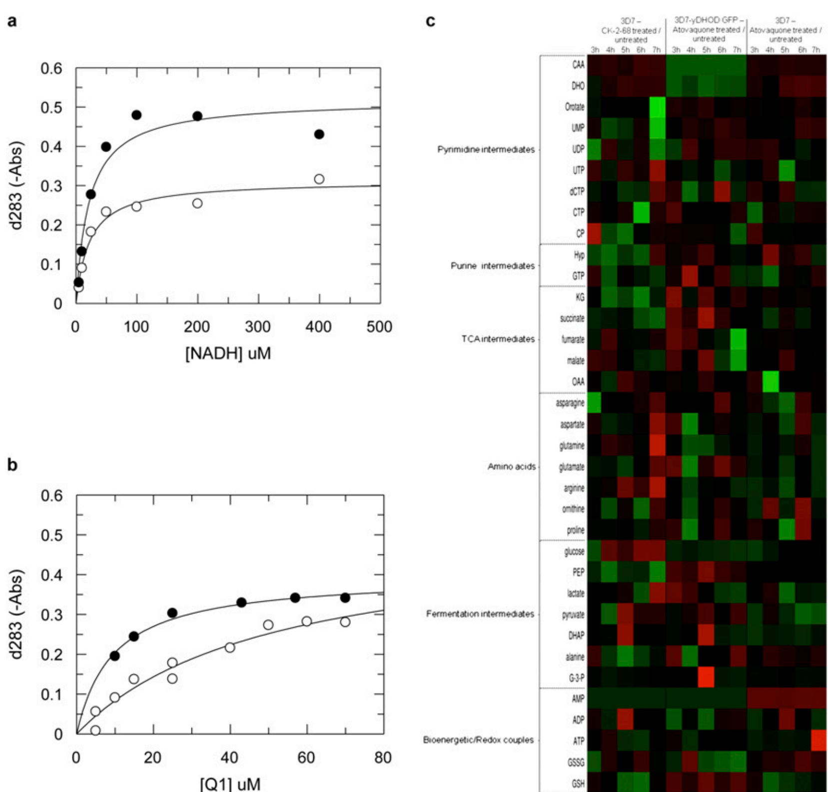

Fig. S4. Nonlinear regression plots showing the steady-state kinetics of PfNDH2 in the presence (○) and absence (●) of CK-2–68 (22 nM) with varying substrate concentrations for (*A*) NADH and (*B*) Q_1. Recombinant PfNDH2 (*E. coli* strain F571) was used as described in *Materials and Methods*. (*C*) Heat map of metabolome dynamics following addition of drug (50 nM CK -2–68 or 2.5 nM atovaquone) to *P. falciparum* 3D7 and 3D7-yDHODH·GFP parasites. Fold changes are relative to untreated controls.

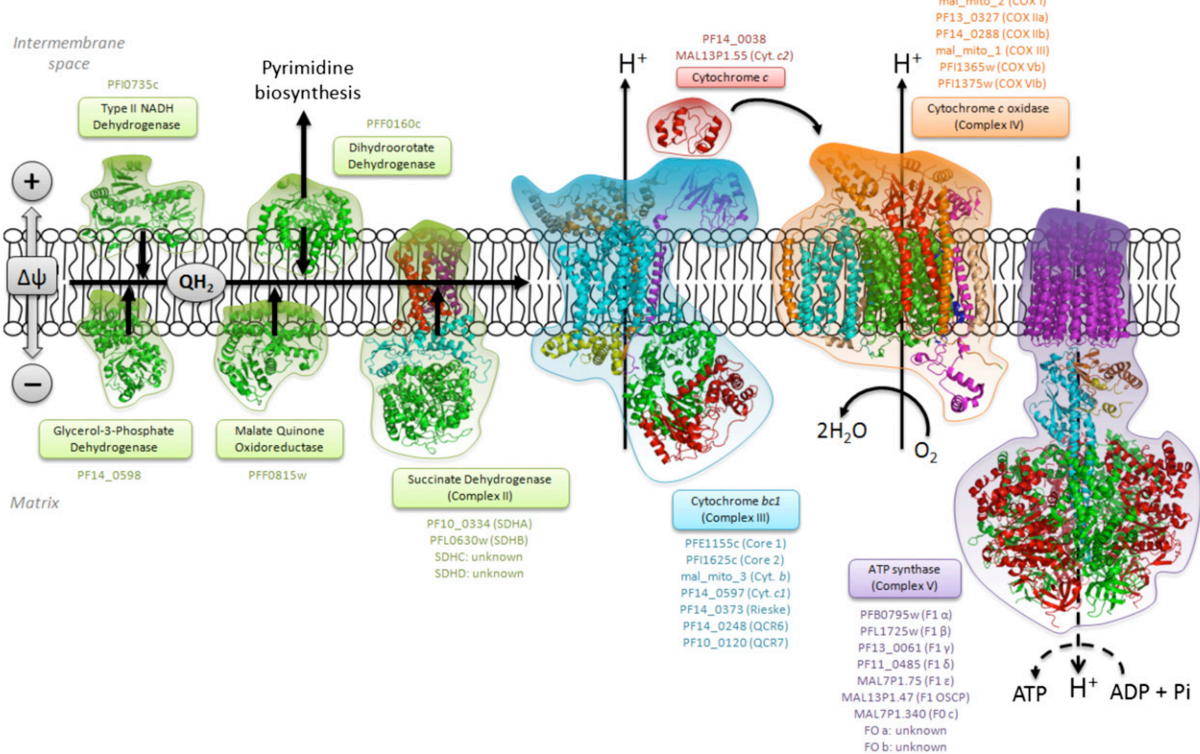

Fig. S5. Predicted mitochondrial electron transport chain (ETC) of *P. falciparum*. The ETC components are drawn as ribbon diagrams of the ortholog structures available in the Protein Data Bank.

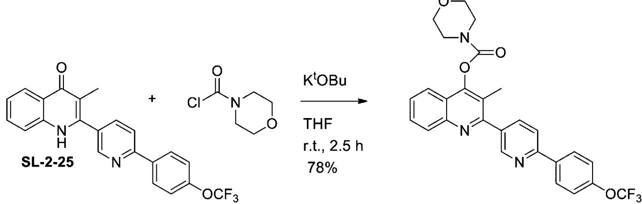

Fig. S6. Synthesis of morpholine carbamate prodrug of SL-2–25.

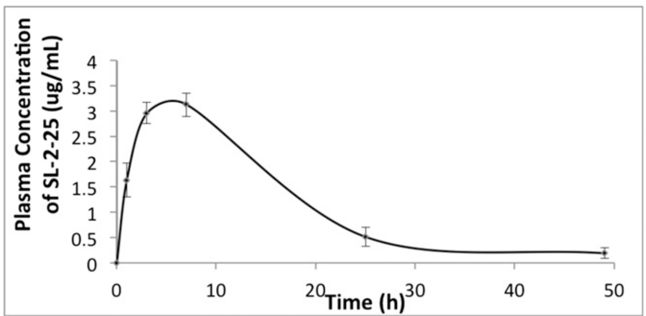

Fig. S7. Concentration-time profile of SL-2–25, in male Wistar rats after oral administration of SL-2–25S phosphate salt (5 mg/kg body weight) (n = 3).

Table S1. Pharmacophores identified from the high throughput screen of the BioFocus library possessing inhibitory activity against recombinant PfNDH2

Substructure	Number of hits	PfNDH2 enzyme inhibition IC_{50} (range in nM)
	4	213–7,448
	17	328–10,471
	2	353–5,250
	1	498
	4	611–6,101
	2	1,190–1,591
	5	1,644–3,740
	4	1,612–10,473
	2	3,623–7,441

Table S2. Inhibitory profile of respiratory chain inhibitors showing differential selectivity for parasite mitochondrial bc_1 and PfNDH2 enzymes

Compound	IC_{50} 3D7 (nM)	IC_{50} PfNDH2 (nM)	IC_{50} bc_1* (nM)	Selectivity (bc_1/PfNDH2)
CK-2–68	31 ± 3	16	500	31
SL-2–34	59 ± 9	<1	38	>38
LT009	83 ± 9	<1	25.5	>25.5
SL-2–64	75 ± 9	4.2	26.8	6.38
CK-2–67	117 ± 27	16	37.5	2.34
SL-2–25	78 ± 8	14.6	15.1	1.03
WDH-1W-5	74 ± 14	49.1	152	3.10

*Cytochrome *c* reductase activity measurements were assayed in 50 mM potassium phosphate, pH 7.5, 2 mM EDTA, 10 mM KCN, and 30 μM equine cytochrome *c* at room temperature. Cytochrome *c* reductase activity was initiated by the addition of decylubiquinol (50 μM). The cytochrome *b* content of membranes was determined from the dithionite-reduced minus ferricyanide-oxidized difference spectra. Inhibitors of bc_1 activity were added without prior incubation.

Table S3. Antimalarial activity of selected compounds against *P. falciparum* strain W2

Compound	Structure	IC_{50} W2 (μM)
RKA070		0.036 ± 0.0005
CK-2–67		0.026 ± 0.0012
CK-2–68		0.017 ± 0.0006
RKA066		0.008 ± 0.0007
PG201		0.148 ± 0.1736
WDH-1U-4		0.042 ± 0.0013
PG221		0.076 ± 0.0018
PG203		0.034 ± 0.0034
CK-3–22 (RKA249)		0.050 ± 0.0025
RKA155		0.067 ± 0.0039
SL-2–25		0.050 ± 0.0127
SL-2–64		0.070 ± 0.0093
SL-2–39		0.088 ± 0.022
SL-3–2		0.12 ± 0.0062
PG128		0.329 ± 0.0412
CK-2–86		3.073 ± 0.1039
RKA271		0.090 ± 0.0041
RKA290		1.267 ± 0.263
RKA304		1.118 ± 0.012
Artemisinin		0.009 ± 0.0011
Chloroquine		0.045 ± 0.0013